Plant Ecol (2011) 212:1855–1871
DOI 10.1007/s11258-011-9959-2

Spatial variation and temporal instability in climate-growth relationships of sessile oak (*Quercus petraea* [Matt.] Liebl.) under temperate conditions

Pierre Mérian · Jean-Daniel Bontemps · Laurent Bergès · François Lebourgeois

Received: 30 March 2011 / Accepted: 12 August 2011 / Published online: 10 September 2011

Abstract Temporal instability of forest climate-growth relationships has been evidenced at high elevations and latitudes, and in Mediterranean contexts. Investigations under temperate conditions, where growth is under the control of both winter frost and summer water stress, are scarce and could provide valuable information about the ability of forest to cope with climate change. To highlight the main climatic factors driving the radial growth of *Quercus petraea* forests and to detect their possible evolutions over the last century, dendroecological analyses were performed along a longitudinal gradient of both decreasing summer water stress and increasing winter frost in northern France (from oceanic to semi-continental conditions). The climate-growth relationships were evaluated from 31 tree-ring chronologies (720 trees) through the calculation of moving correlation functions. *Q. petraea* displayed a rather low sensitivity to climate. High temperature in March and water stress from May to July appeared to be the main growth limiting factors. The sensitivity to winter precipitation and summer water stress decreased from oceanic to semi-continental conditions, whilst the correlation to winter frost tended to increase. Moving correlations revealed a general instability of climate-growth relationships, with a moderate synchronicity with climatic fluctuations. The main changes occurred during previous autumn for both temperature and precipitation whilst climatic trends were rather low or non-significant. The most coherent trends were pointed out (i) in April with a cooling (−0.9°C) leading to positive correlation to temperature at the end of the century, and (ii) in July with a decreasing inter-annual variability of precipitation resulting in a loss of correlation. On the contrary, the decreasing temperature and increasing precipitation in May and June led to few significant changes climate-growth relationships.

Keywords Dendroecology · Climate variability · *Quercus petraea* · Temperate forests · Temporal instability · Correlation functions

Electronic supplementary material The online version of this article (doi:10.1007/s11258-011-9959-2) contains supplementary material, which is available to authorized users.

P. Mérian (✉) · J.-D. Bontemps · F. Lebourgeois
AgroParisTech, ENGREF, UMR 1092 INRA/AgroParisTech Laboratoire d'Etude des Ressources Forêt-Bois (LERFoB), 14 rue Girardet, 54000 Nancy, France
e-mail: pierre.merian@engref.agroparistech.fr

P. Mérian · J.-D. Bontemps · F. Lebourgeois
INRA, Centre de Nancy, UMR 1092 Inra/AgroParisTech Laboratoire d'Etude des Ressources Forêt-Bois (LERFoB), 54280 Champenoux, France

L. Bergès
Cemagref, UR EMAX, Centre d'Aix en Provence, CS 40061, Aix en Provence Cedex 5, France

Introduction

Climate models predict a global warming and a modification of the precipitation regime distribution throughout Europe (Jones and Moberg 2003; Moberg and Jones 2005; Briffa et al. 2009), including France (Moisselin et al. 2002). Mean annual temperature will increase between 2 and 4.5°C until the end of the 21th century, accompanied by a 35–45% decrease in summer precipitation, suggesting increases in drought frequency and severity. In the context of climatic change, questions have arisen concerning forest composition, survival and growth in response to changes in yearly weather conditions and/or extreme events (Rotzer et al. 2005; Lindner et al. 2010).

Recently, many tree-ring studies have highlighted a decreasing response of forest ecosystems to temperature since around the middle 20th century at high elevations and latitudes (D'Arrigo et al. 2008), and an increasing sensitivity to summer water balance in temperate (Friedrichs et al. 2009a) or in Mediterranean (Tardif et al. 2003; Macias et al. 2006; Andreu et al. 2007) contexts, called "divergence". The divergence is defined as "a change in climate sensitivity and/or a divergence in trend" (D'Arrigo et al. 2008). Whilst the underlying mechanisms are still largely debated, these trends have been mainly attributed to climatic change (D'Arrigo et al. 2008). Such changes in climate control contradict the uniformitarian principle traditionally applied to dendroclimatology (Fritts 1976), and may have important consequences for the utilisation of tree-ring records in temperature reconstructions (Hughes 2002) or carbon uptake projections (Davi et al. 2006). The overview of D'Arrigo et al. (2008) has also underlined that little is known about the European low-altitude temperate forests and especially for the main broad-leaved ecosystems. In these contexts, forest growth is under the control of both winter frost and summer water stress; their respective influence varying throughout the growing season and according to the local ecological conditions (Lebourgeois et al. 2005; Friedrichs et al. 2009b). As a result of this multiple growth control, various response patterns to environmental changes can be hypothesized. Thus, analysing the variation of climate influences on radial growth appeared to be a powerful tool to provide valuable information about the forest sustainability (Biondi 1997).

In Europe, three deciduous species dominate lowland temperate forests: sessile oak (*Quercus petraea* [Matt.] Liebl.), pedunculate oak (*Q. robur* L.) and common beech (*Fagus sylvatica* L.). Whilst the response to climate variability of the two latter species has been thoroughly studied in Europe under a wide range of climatic contexts (Tessier et al. 1994; Kelly et al. 2002; Dittmar et al. 2003; Piovesan et al. 2005; Rozas 2005; Di Filippo et al. 2007; Friedrichs et al. 2009b), specific studies on *Q. petraea* have been scarcer and limited to small-scale zones. The more recent ones were led in central Europe (Friedrichs et al. 2009a, b; Dolezal et al. 2010), and in western (Lebourgeois et al. 2004) and southern France (Tessier et al. 1994; Misson et al. 2004). All of them pointed out a low response to climate, even if summer water stress appeared to be the primary limiting factor of radial growth. Under semi-continental conditions, Friedrichs et al. (2009a) showed a strengthening of the positive correlation between radial growth and drought indexes throughout the 20th century, even if the radial growth strongly increased during the exceptionally warm and dry 1940s. Only Kelly et al. (2002) provided a pan-European perspective, but limited to climatic factors driving extreme growth years; the growth reductions were associated with low temperature or high water stress. Thus, the large-scale variations of climate-growth relationships of *Q. petraea* under temperate conditions and their temporal evolutions remained largely misunderstood.

This study sought to investigate spatio-temporal changes of climate-growth relationships of *Q. petraea* at broad scale and over the 20th century. Forests were sampled in northern France, under a wide range of climatic contexts representing the weather conditions observable in a large part of Western and Central Europe. The West-East climatic gradient coincided with both decreasing temperature and increasing precipitation, implying a decreasing water stress and increasing winter frost. Our hypotheses were that (1) a decreasing limitation of summer water stress and an increasing limitation of winter frost may be evidenced from West to East, and (2) temporal changes in climate-growth relationships may be spatially dependent, with an increasing correlation to summer water stress under oceanic conditions and a decreasing one to winter frost under semi-continental climate.

Materials and methods

Study area

The study area covered the northern half of France between 46.10° to 49.02°N and 1.32°W to 7.43°E (Fig. 1), under a wide range of bioclimatic conditions, from oceanic to semi-continental climate (from West to East). This longitudinal gradient coincided with both increasing precipitation and decreasing temperature. Oceanic climate was characterized by low thermal amplitude due to mild winters and fresh summers, and intermediate precipitation level (Fig. 2a). Semi-continental climate corresponded to lower mean annual temperature, and higher precipitation and thermal amplitude with cold winters (Fig. 2b).

To characterize the extreme climatic events, the frequencies of drought and frost were calculated per month. A drought event was defined according to the Gaussen and Bagnoul Aridity Index (Gaussen and Bagnouls 1952), whilst a frost event corresponded to a mean monthly temperature below zero. Under oceanic conditions, the drought frequency was found to be around twice higher from May to August compared to semi-continental ones (Fig. 2). On the contrary, the frost frequency was twice higher under semi-continental during winter (from December to February).

Sampling, ring width measurement and chronology building

The samples came from three different data-sets, for a total of 120 sampled plots composed of pure and even-aged stands (Duplat and Tran-Ha 1997; Lebourgeois 1997; Bergès et al. 2000). At each plot, 2–30 dominant trees were cored to the pith at breast height with an increment borer between 1993 and 2001 (one core per tree, 720 trees). The general topography was gently rolling (slope < 20%) with elevation ranging from 57 to 380 m a.s.l.

Depending on the data-set, two methods were used to measure the ring widths: 20% were measured with

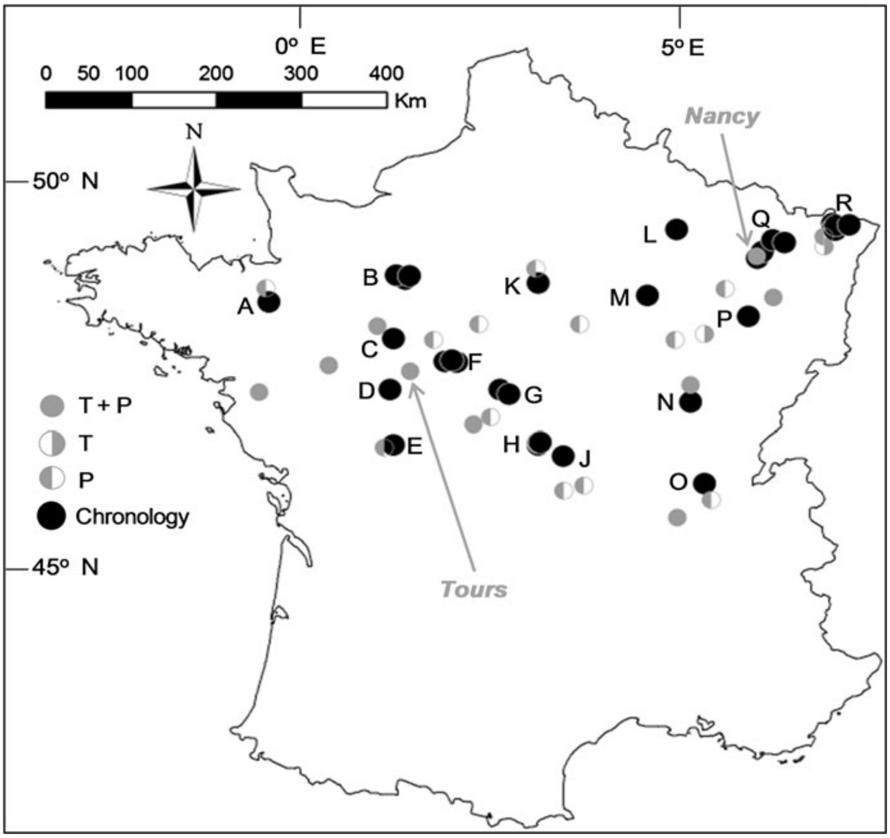

Fig. 1 Geographical location of the 31 chronologies (*black circles*) and the 24 meteorological stations (*grey circles*: series of temperature and precipitation, *white–grey circles*: series of temperature, *grey-white circles*: series of precipitation). *T* temperature; *P* precipitation

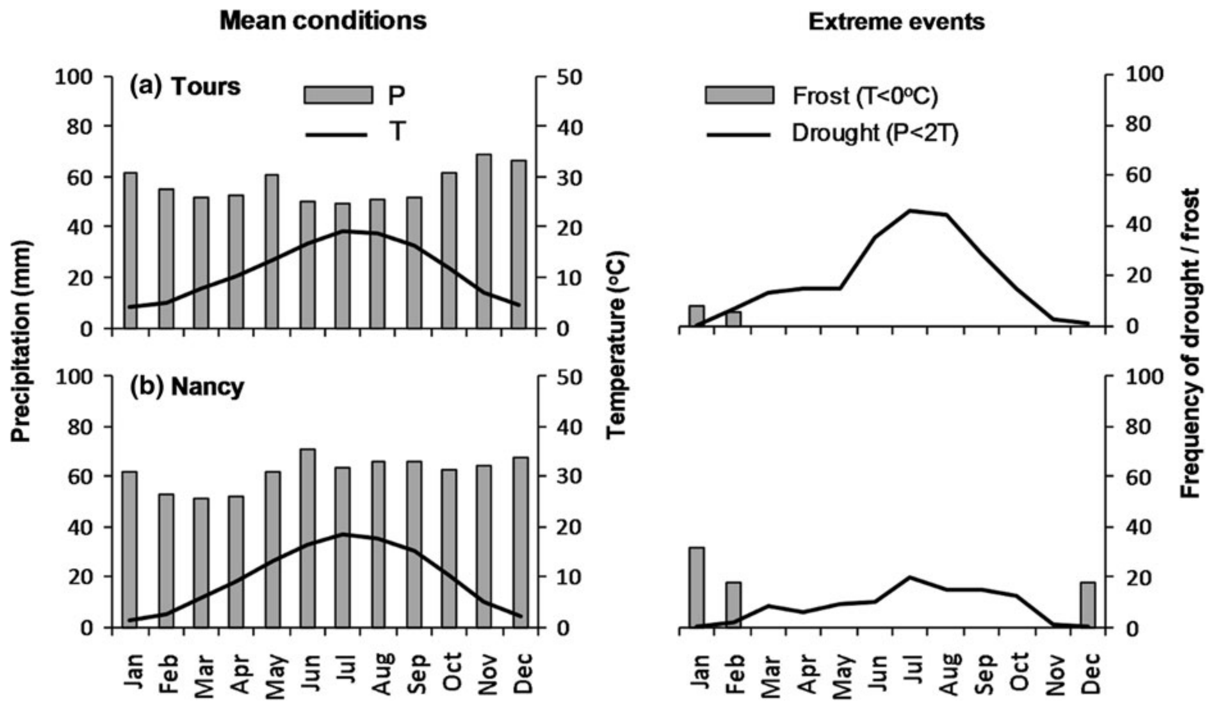

Fig. 2 Mean conditions (*left*) and extreme events (*right*) for Tours (**a**: 47°26′36″ N, 00°43′36″ W, 108 m) and Nancy (**b**: 48°41′12″ N, 06°13′18″ W, 212 m). Geographical locations in Fig. 1. Climatic diagram: mean monthly temperatures (°C; *black line*) and precipitation (mm; *grey bars*). Extreme events: frequencies of frost ($T < 0$°C; *grey bars*) and drought ($P < 2T$; *black line*). Climatic values were calculated for the period 1914–1993

an X-ray method to the nearest 0.025 mm, 50% with a stereo-microscope connected to a micro-computer and the tree-ring program SAISIE to the nearest 0.01 mm (Becker 1989) and 30% with both methods. The X-Ray method relied on measuring ring width in a single direction from the pith to the cambium, whilst the stereo-microscope one defined ring width in a direction orthogonal to the ring tangents. Thus, for a given ring, the X-Ray method gave systematically a higher width. To ensure homogeneity of tree-ring data, the ring widths obtained with the X-ray method were converted into measurements comparable to those performed with the stereo-microscope, using the following equation established on rings measured with both methods ($n = 23868$):

$$W_{\text{microscope}} = 1.1649(W_{\text{X-Ray}}) - 0.1491 \quad (1)$$

where $W_{\text{X-Ray}}$ and $W_{\text{microscope}}$ are the ring widths measured with the X-ray method and the stereo-microscope, respectively ($R^2 = 0.762$, $P < 10^{-9}$).

The effect of this conversion on climate-growth relationships was investigated through the calculation of bootstrapped correlation functions with initial and converted ring widths. The difference between the two sets of bootstrapped correlation coefficients (BCC) was tested with a paired t test run on $\text{BCC}_{\text{X-Ray}}$ and $\text{BCC}_{\text{X-Ray converted}}$, i.e. the BCC calculated on the ring widths measured with the X-ray method and then corrected with the Eq. 1. The conversion did not significantly affect the climate-growth relationships at the level of 5% (Online Resource 1).

The individual ring width series were carefully cross dated by progressively detecting regional pointer years (Schweingruber 1996), which were defined as those calendar years when at least 75% of the cross dated trees presented an absolute value of radial growth variation (RGV) higher than 10% (Becker et al. 1994; Mérian and Lebourgeois 2011). Absolute dating was checked by the application INTERDAT (Becker 1989; Becker and Dupouey unpublished) which identifies locations within each ring series that may have erroneous cross dating. Using the R software (R Development Core Team 2010) and the “dplR” package (Bunn 2008), the tree-ring series were computed on the maximum common period (1914–1993; 80 years) and standardized individually to emphasize the inter-annual climatic signal. A double-detrending process was thus applied, based on an initial negative exponential or linear regression followed by a fitting of a cubic smoothing spline with 50% frequency response cut-off and with a rigidity of 33% of series length (Cook and Peters 1981). Dimensionless indices were obtained by dividing the observed ring width value by the predicted one. This process created stationary time series for each tree with a mean of 1 and a homogeneous variance.

To accurately assess the strength of climate-growth relationships by minimising the noise of each individual detrended series (Fritts 1976; Cook and Kairiukstis 1990), the series from nearby plots were grouped in respect of (i) ecological and dendrometrical characteristics, and (ii) the method of measurement (either X-ray or microscopic), to reach at least 14 trees per chronology (mean = 23). 31 groups of plots were defined, with a distance between 2 grouped plots averaging 9.7 km (standard-deviation: 10.6 km), from which 31 chronologies were established by averaging the growth indexes by year using a bi-weighted robust mean (Cook and Peters 1981). The mean sensitivity and the first-order auto-correlation coefficient were calculated on the detrended data for each tree and averaged per chronology to measure the year-to-year variability and the influence of growth of the previous year on the current year growth, respectively (Fritts 1976). The expressed population signal (EPS) was also calculated to quantify how well the average of individual series represented the population average (Wigley et al. 1984).

Climatic data building

The mean monthly temperature (*T*) and sum of precipitation (*P*) were obtained from 24 meteorological stations of the French National Climatic Network (Météo-France), which presented recordings from September 1913 to August 1993 (Fig. 1). As the mean distance between the sampled plots and the meteorological stations was 53 and 37 km for temperature and precipitation, respectively (standard-deviations: 29 and 22 km), the climatic series were corrected to be as representative as possible of the local weather conditions. In a first step, the mean monthly climatic conditions on the period 1961–1990 were calculated for each meteorological station. In a second step, the same climatic values were extracted per chronology from the AURELHY map at a 1 km^2 resolution (Benichou and Le Breton 1987). The mean monthly climatic differences between meteorological stations and chronology locations were then estimated, and averaged 0.14°C and 2.1 mm for temperature and precipitation. Finally, for each chronology, the climatic series of the nearest meteorological station were corrected according to these mean monthly differences.

Climate-growth analysis

Climate-growth relationships over the 80-year period were investigated through the calculation of correlation functions using chronologies as dependant variables (Guiot 1991) and 24 monthly climatic regressors (12 *T* and 12 *P* values) organised from September of the previous growing season to August of the year in which the ring was formed. The BCC were calculated using the package "bootRes" (Zang 2009). To detect to which extent sensitivity to climate differed amongst the chronologies, two principal component analyses were performed (PCA): the first one on the RGV of the pointer years to highlight variations in response to extreme events (PCA_{PY}) (Lebourgeois et al. 2010b), and the second one on the BCC to point out differences in mean response to climate (PCA_{BCC}) (Tessier et al. 1994; Weber et al. 2007). Both of them were calculated from the variance–covariance matrix since descriptors (either RGV or BCC) were of the same kind and shared the same order of magnitude (Legendre and Legendre 1998). The similarity metric of the PCA was the Euclidean distance.

The temporal variation of the climate-growth relationships was analysed with the moving correlation functions, considering a 24-year fixed interval. Thus, 57 successive periods were defined by increasing the initial and final years of the interval by one per iteration. The temporal variations of climatic regressors were evaluated by the calculation of the mean value (MV) and the standard deviation (SD) for each period. The MV and SD series corresponded to the temporal variation of mean conditions and inter-annual variability, respectively, and were thus interpreted in terms of low- and high-frequency climatic signals. The significance of the BCC, MV and SD trends were tested with the Spearman's rank correlation coefficient (Myers and Well 2003). Because two successive 24-year periods presented 23 common years, BCC, MV and SD values were highly correlated from one to the next. This great inter-correlation was expected to induce mathematical significant trends. To avoid these "false positive" trends, the significance level was set at P-value $< 10^{-4}$.

Results

Descriptive statistics

The mean level of growth (W) varied from 1.33 to 2.50 mm (Table 1) and decreased with increasing age:

$$W = -0.0106\ (\text{Age}) + 2.9912 \quad (2)$$

where W is the mean ring width per plot on the period 1914–1993 (in mm) and Age the mean age of trees per plot in 1993 ($R^2 = 0.548$, $P < 10^{-5}$).

On the contrary, the mean tree age was not significantly correlated to the chronologies location along the longitudinal gradient ($R^2 < 0.01$), implying that the spatial variation of the climatic response was not influenced by tree age. The mean sensitivity ranged from 0.12 to 0.21 (mean = 0.16) and was negatively correlated to mean tree age ($R^2 = 0.156$, $P = 0.034$). The first-order autocorrelation coefficient varied between 0.17 and 0.59, pointing out a strong dependence of current growth on the previous year's growth. All EPS values exceeded the threshold of 0.85 which supported the conclusion that the signal of the chronologies was representative of the population signal (Wigley et al. 1984).

Response to extreme events

For the period 1914–1993, the number of pointer years ranged from 10 to 33, and averaged 22 (Table 1). The mean number of positive and negative years was similar, with average RGV of 45 and −26%, respectively. The number of pointer years increased with increasing mean sensitivity and EPS (Table 1), whilst the RGV remained stable (Online Resource 2).

The two first axes of the PCA_{PY} explained 32.3 and 12.8% of the total inertia. All chronologies presented positive scores on the first axis, revealing a common pattern in the response to extreme events (Fig. 3a). In the negative direction, the main structuring years were 1921, 1933 and 1976 (Fig. 3b), corresponding to exceptional drought events during late spring or summer (Online Resource 2). Sessile oak reacted commonly and negatively to these extreme years (−21, −20 and −25%, respectively). In the positive direction, the main years were 1946, 1958 and 1982 with particularly fresh and wet springs/summers. Trees responded positively, with mean RGV of 30, 47 and 51%, respectively. The second axis gave evidence of local extreme events along the longitudinal gradient, scores decreasing with increasing longitude ($R^2 = 0.760$, P-value $< 10^{-6}$). For example, the drought events in 1934 and 1989 were mainly located in the West, whilst those of 1915 and 1947 were restricted to the East (Fig. 3b and Online Resource 2).

In general, pointer years were highly related to late spring and summer conditions, warm and dry years leading to a decrease of the ring width. However, in 1956, sessile oak growth was limited by winter frost with a mean deviation of −8.7 to −10.1°C in February compared to the long-term monthly mean (Online Resource 2).

Spatial variation in climate-growth relationships

The PCA_{BCC} showed that the variation in sensitivity to climate strongly reflected the spatial distribution of the chronologies (Fig. 4a). The first axis ($PC_{BCC}1$) represented 31.2% of the total inertia; the scores of the 31 chronologies were greatly and significantly correlated to the longitude ($R^2 = 0.850$). The main structuring climatic variables were related to winter (December to March) and summer (June to August) conditions, with positive scores for temperature and negative for precipitation (Fig. 4b). The second axis represented 18.3% of the total inertia and was not correlated to the geographical location of the chronologies. $PC_{BCC}2$ mainly distinguished the chronologies sampled in the North-West which displayed a weak sensitivity climate, except in previous November and December with a strong and positive correlation to precipitation (Fig. 4b). This pattern agreed with the high autocorrelation and low mean sensitivity values observed for these chronologies (Table 1).

The general spatial variation in climate-growth relationships consisted first in a West to East decrease

Table 1 Climatic characteristics and descriptive statistics of the 31 chronologies from 1914 to 1993

Chr.	Coordinates			Climate										Descriptive statistics							
	Longitude	Latitude	Alt.	Temperature			Precipitation		Frost freq.		Drought freq.			Nb. tr (nb. pl)	Age	*W* (mm)	MS	AC	EPS	NPY	PPY
				Year	Jan.	MJJ	Year	MJJ	Jan.	Feb.	May	June	July								
A	1°32′05″W	48°10′37″ N	80	11.8	4.83	16.5	727	154	3	3	14	33	40	28 (1)	99 (7)	2.05 (0.72)	0.15	0.53	0.97	9	11
B1	0°36′47″ E	48°29′06″ N	242	10.9	3.08	16.1	695	159	10	5	14	30	31	20 (7)	143 (41)	1.49 (0.62)	0.14	0.59	0.92	6	9
B2	0°28′10″ E	48°31′41″ N	250	10.9	3.82	15.6	689	162	9	5	14	23	30	18 (6)	124 (20)	1.64 (0.66)	0.15	0.59	0.95	7	15
B3	0°40′46″ E	48°31′21″ N	220	11.0	3.73	15.6	674	159	9	5	14	28	28	30 (1)	85 (2)	1.75 (0.62)	0.17	0.53	0.98	12	14
C	0°27′19″ E	47°48′46″ N	126	11.2	3.66	16.6	672	161	5	4	13	30	34	27 (10)	95 (13)	2.13 (0.85)	0.13	0.45	0.96	8	7
D	0°25′20″ E	47°14′16″ N	96	11.0	3.08	16.7	670	155	6	4	13	30	44	15 (5)	107 (14)	1.81 (0.64)	0.12	0.37	0.86	4	6
E	0°29′40″ E	46°37′36″ N	116	10.7	2.80	16.5	691	162	11	6	11	31	41	28 (1)	81 (4)	1.89 (0.81)	0.21	0.38	0.97	13	15
F1	1°15′33″ E	47°34′07″ N	127	10.8	2.73	16.7	649	158	11	5	15	26	36	30 (1)	90 (7)	2.05 (0.77)	0.20	0.32	0.97	15	14
F2	1°26′38″ E	47°33′43″ N	102	10.7	2.58	16.4	648	158	13	6	15	28	36	18 (6)	117 (32)	2.02 (0.83)	0.20	0.31	0.95	16	16
F3	1°22′34″ E	47°34′50″ N	117	11.0	2.81	16.7	646	158	11	5	15	28	38	17 (6)	115 (23)	1.63 (0.60)	0.15	0.44	0.94	9	8
G1	2°07′28″ E	47°15′14″ N	176	10.9	2.98	16.5	686	175	13	5	11	21	35	23 (1)	78 (8)	2.35 (0.88)	0.19	0.22	0.95	16	12
G2	2°16′12″ E	47°12′27″ N	179	10.9	3.00	16.5	686	175	13	5	11	21	35	15 (6)	103 (18)	2.06 (0.69)	0.15	0.34	0.92	12	7
H1	2°43′27″ E	46°38′11″ N	267	11.0	3.06	16.5	693	203	10	6	6	11	33	18 (6)	116 (29)	1.47 (0.52)	0.14	0.44	0.91	8	6
H2	2°43′35″ E	46°40′01″ N	260	11.2	3.06	16.5	695	202	10	6	6	11	33	30 (1)	111 (6)	1.68 (0.61)	0.15	0.41	0.97	14	13
H3	2°45′32″ E	46°40′14″ N	254	10.8	3.06	16.5	694	203	10	6	6	11	33	14 (5)	137 (40)	1.75 (0.60)	0.12	0.42	0.89	4	6
J	3°06′41″ E	46°30′38″ N	282	11.1	3.14	16.8	710	221	10	6	5	10	33	15 (5)	134 (35)	1.79 (0.63)	0.14	0.39	0.88	7	7
K	2°43′43″ E	48°27′10″ N	80	10.8	3.25	16.4	640	165	13	9	18	20	25	29 (1)	108 (4)	1.85 (0.79)	0.18	0.35	0.96	14	9
L	4°57′36″ E	49°01′58″ N	180	9.4	0.90	15.4	829	210	31	18	8	9	20	26 (1)	137 (22)	1.60 (0.68)	0.17	0.43	0.96	12	13
M	4°27′34″ E	48°17′50″ N	160	9.9	0.98	15.8	809	204	26	15	6	10	25	24 (1)	84 (6)	2.00 (0.82)	0.20	0.39	0.97	15	18
N	5°04′27″ E	47°04′56″ N	220	10.7	1.52	16.7	781	207	19	8	5	11	26	30 (1)	84 (5)	2.27 (0.95)	0.15	0.58	0.96	10	12
O	5°14′18″ E	46°10′14″ N	260	11.3	2.06	17.1	821	244	18	9	8	10	28	30 (1)	85 (8)	1.91 (0.66)	0.16	0.25	0.95	11	13
P	6°02′22″ E	48°01′33″ N	330	9.4	0.83	15.3	922	234	35	20	6	8	13	30 (1)	127 (19)	1.48 (0.60)	0.18	0.39	0.96	11	15
Q1	6°13′39″ E	48°40′24″ N	286	10.2	1.25	15.8	756	198	28	16	10	13	25	18 (6)	104 (13)	2.05 (0.80)	0.17	0.49	0.94	10	12
Q2	6°18′18″ E	48°44′31″ N	266	9.8	1.18	15.8	792	205	28	18	9	10	21	19 (7)	103 (18)	2.15 (0.92)	0.17	0.45	0.93	10	15
Q3	6°29′39″ E	48°52′18″ N	315	9.7	1.06	15.7	847	220	31	18	5	8	16	30 (1)	83 (3)	2.18 (0.80)	0.18	0.40	0.98	14	15
Q4	6°40′30″ E	48°49′58″ N	275	9.6	0.99	15.6	870	224	33	18	5	6	15	15 (6)	80 (8)	2.50 (1.09)	0.16	0.46	0.93	8	8
R1	7°27′40″ E	49°00′56″ N	320	9.7	0.91	16.0	819	221	36	19	6	5	16	29 (1)	127 (6)	1.33 (0.44)	0.16	0.27	0.97	12	13
R2	7°27′55″ E	48°57′19″ N	333	9.6	0.89	15.9	824	223	36	19	6	5	18	24 (8)	129 (31)	1.60 (0.63)	0.15	0.28	0.95	13	12
R3	7°30′67″ E	48°56′34″ N	318	9.5	0.89	15.9	818	222	36	19	6	5	16	29 (10)	107 (24)	2.06 (0.81)	0.14	0.18	0.94	11	8

Table 1 continued

Chr.	Coordinates		Alt.	Climate											Descriptive statistics							
	Longitude	Latitude		Temperature			Precipitation		Frost freq.		Drought freq.				Nb. tr (nb. pl)	Age	*W* (mm)	MS	AC	EPS	NPY	PPY
				Year	Jan.	MJJ	Year	MJJ	Jan.	Feb.	May	June	July									
R4	7°30′50″ E	48°59′28″ N	346	9.5	0.91	16.0	810	221	36	19	6	5	16		17 (6)	118 (25)	1.51 (0.76)	0.19	0.17	0.94	15	14
R5	7°43′43″ E	48°59′22″ N	350	9.9	0.94	16.0	783	217	34	19	9	6	19		24 (1)	76 (3)	1.99 (0.80)	0.16	0.44	0.95	10	13

MS and AC were calculated on the detrended data. Bold names of chronologies indicate chronologies resulting from a grouping of plots

Mean (standard deviation). *Chr.* chronology; *Alt.* altitude (m); *Jan.* January; *Feb.* February; *MJJ* May–June–July; Age in 1993; *Nb.tr* (*nb. pl*) number of trees (number of plots); *W*: ring width (mm); *MS* mean sensitivity; *AC* first-order auto-correlation coefficient; *EPS* expressed population signal; *NPY* number of negative pointer years; *PPY* number of positive pointer years

in the positive correlation to precipitation from previous November to current March (Fig. 5a). Chronologies responded significantly under oceanic conditions, whilst slightly non-significant negative correlations were observed in December and January in the most eastern part of the area (Fig. 5b). These chronologies also displayed a positive but non-significant correlation to winter temperature. In a second time, significant correlations were found between sensitivity to autumn/winter temperature and the longitude. From West to East, BCC were more and more positive in October and January, and changed from positive to negative values in November. Finally, strong differences were evidenced from June to August for both temperature and precipitation. In June, the pattern consisted in an increasing sensitivity to drought from West to East, i.e. more negative BCC to temperature and positive to precipitation (Fig. 5c). The opposite trend was found in July and August, with a lower sensitivity to *T* and *P* under semi-continental conditions (Fig. 5d).

For some climatic regressors, BCC were consistent over the 31 chronologies. Response to temperature from February to May was generally non-significant, except in March with a common and negative correlation (Fig. 5a). Similarly, sensitivity to precipitation in previous autumn (September and November) was very weak, whilst precipitation in May positively influenced the radial growth.

Temporal variation in climate-growth relationships

Climatic trends

The observed climatic trends (i.e. MV and SD) over the period 1914–1993 were highly similar between the 31 chronologies for both sign and intensity (Online Resource 3), and were thus presented at the scale of the study area (Fig. 6a). For temperature, the overall trend corresponded to a cooling from March to June, and in September. No significant changes were found from November to February and in late summer. The strongest decrease was observed in April (−0.91°C), whilst the other ones ranged from −0.29 to −0.52°C. In the same way, SD significantly decreased in spring (−0.35 to −0.39°C), but also in late summer (August and September: −0.25), and in November (−0.27).

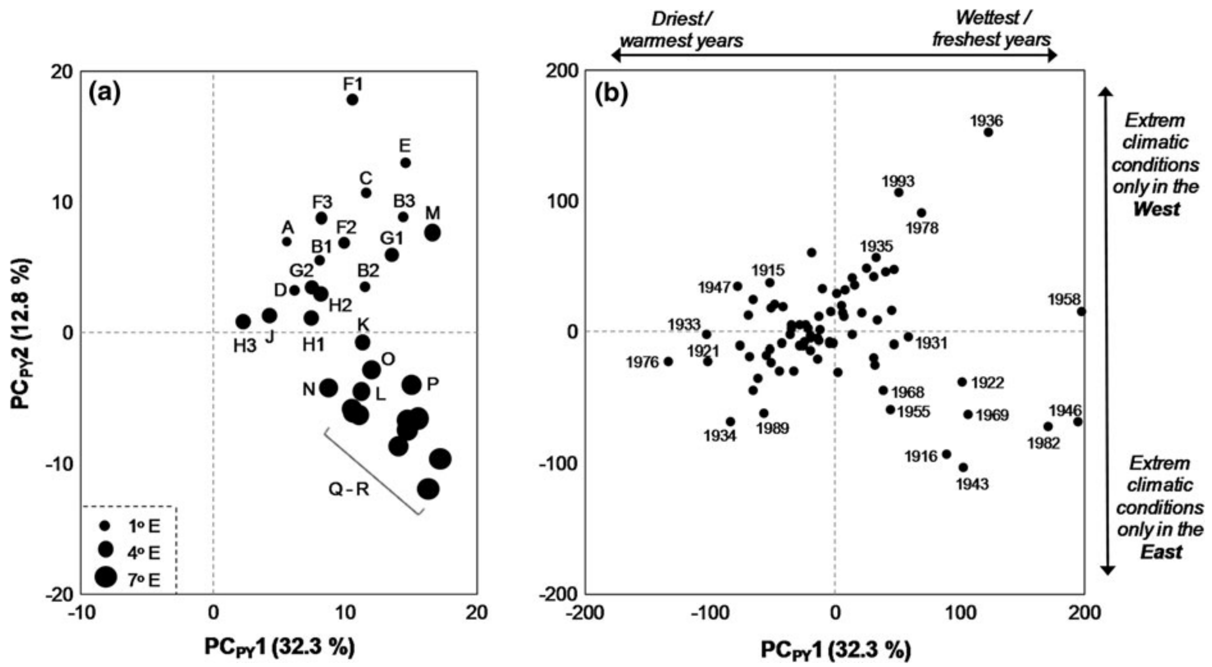

Fig. 3 Scatter plots of the principal component analysis loaded on the pointer years calculated on the period 1914–1993. **a** Chronologies, increasing circle size with increasing longitude; **b** years. Results are presented on the two first components

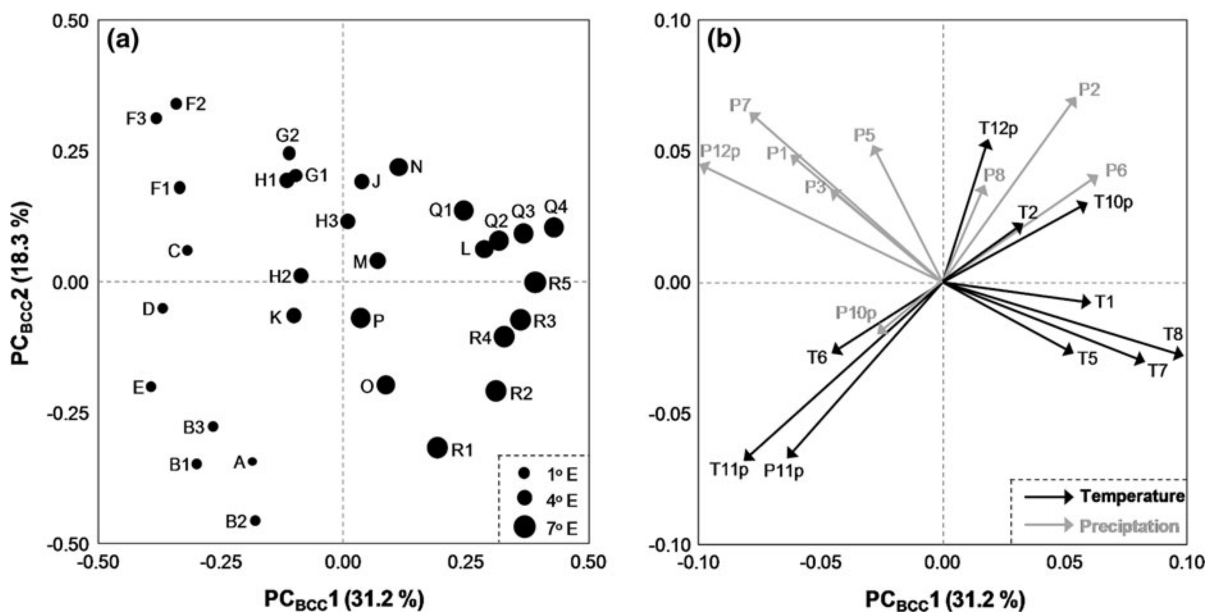

Fig. 4 Scatter plots of the principal component analysis loaded on the bootstrapped correlation coefficients calculated on the period 1914–1993. **a** Chronologies, increasing circle size with increasing longitude; **b** climatic regressors. *Black arrows*: temperature; *grey arrows*: precipitation; *T* Temperature; *P* Precipitation; month is represented by a *number* (e.g. 1: January); *p*: year before ring formation (year $n - 1$). Results are presented on the two first components

Except in April, precipitation significantly increased from winter to early summer (+4 to 11 mm), and became also more variable (+4 to 7 mm). During July and October, opposite trends were observed, with decreasing MV for both months (−10 and −16 mm) and SD only in July (−10 mm).

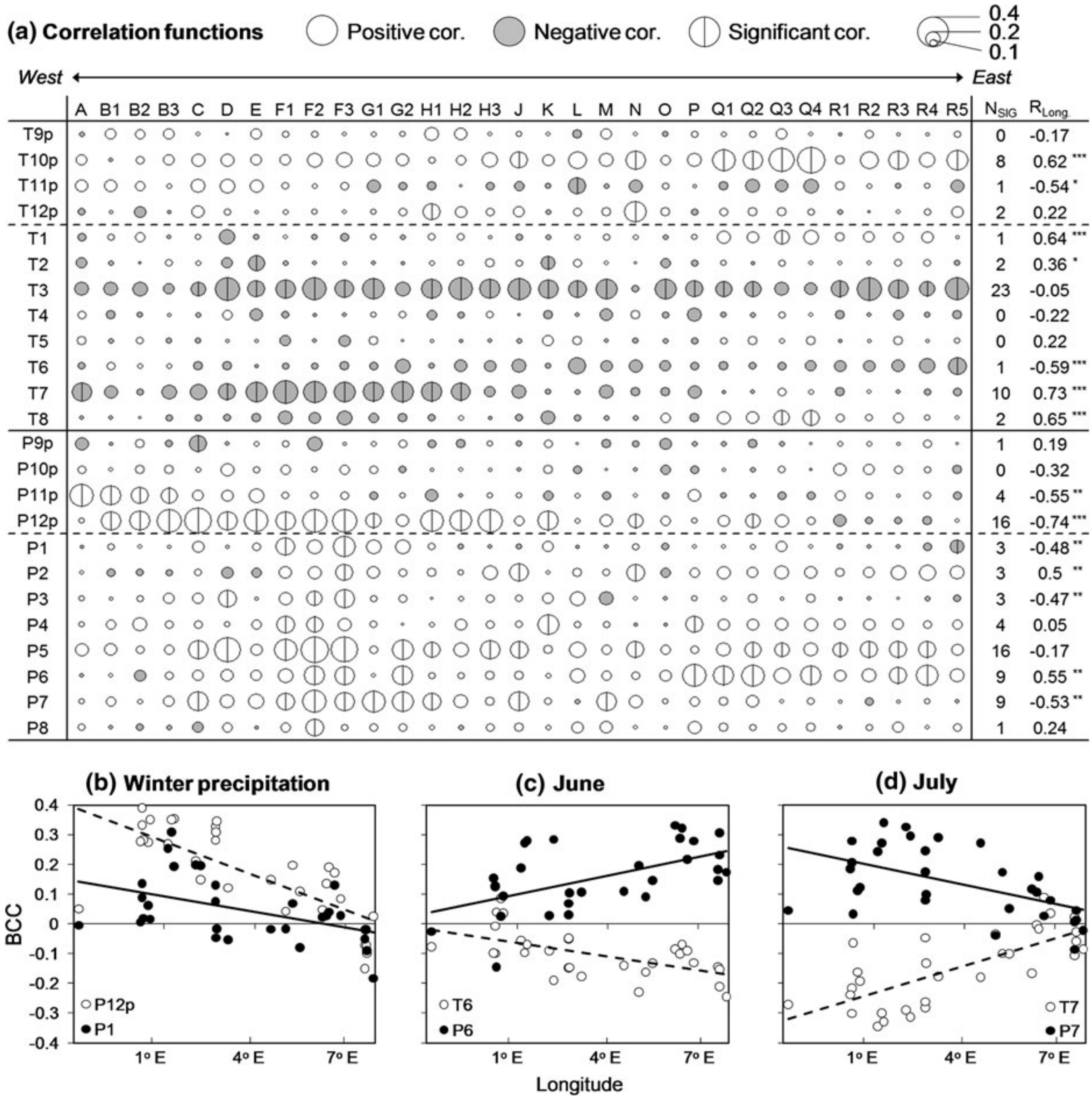

Fig. 5 **a** Correlation functions of the 31 chronologies classified according to the longitude (from West to East). *Open circles* positive bootstrapped correlation coefficients (BCC); *grey circles* negative BCC; *vertical lines* significant BCC ($P < 0.05$); increasing circle size with increasing correlation; *T* temperature; *P* precipitation; month is represented by a *number* (e.g. 1: January); *p* year before ring formation (year $n - 1$); N_{SIG} number of significant responding chronologies per climatic regressor; R_{Long}: correlation coefficient between BCC and longitude values (*asterisks* denote the significant levels: *< 0.05, **< 0.01, ***< 0.001). **b**, **c**, **d**: graphs representing the same data for three cases: winter precipitation (December and January), June and July, respectively

In conclusion, temperature became cooler and less variable during spring and early summer from 1914 to 1993. Precipitation tended to increase with a higher year-to-year variability, except during July and mid-autumn.

BCC trends

Moving correlation functions revealed significant variations of BCC for the 24 climatic regressors (Fig. 6a). Indeed, Spearman's rank correlation

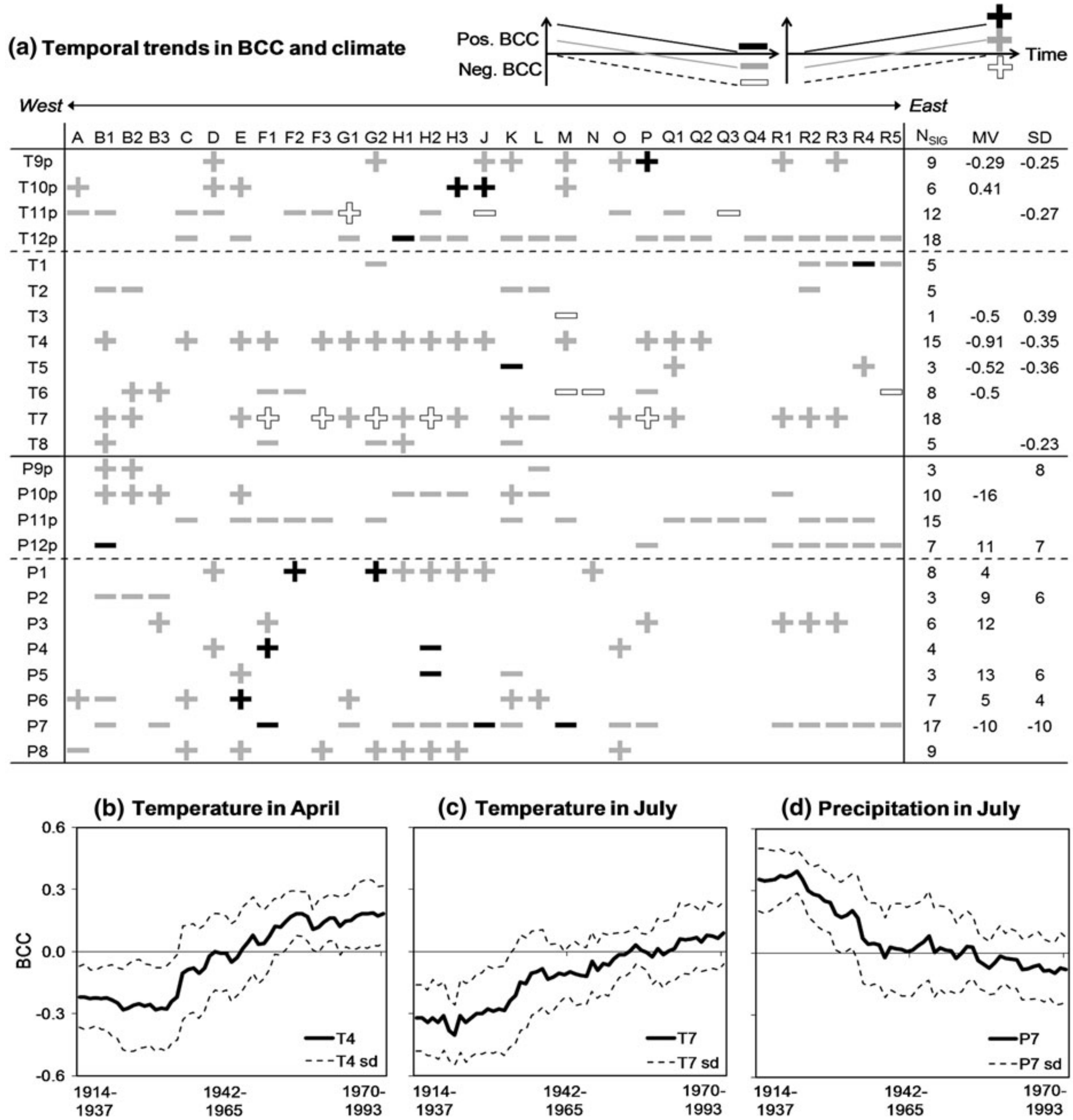

Fig. 6 **a** Significant temporal changes of bootstrapped correlation coefficients (BCC) and climatic regressors amongst the 57 successive periods (Spearman's rank correlation coefficient, level of significance: 0.0001). Symbols "+" and "−" indicate increasing and decreasing BCC, respectively. *Black symbols* indicate positive BCC, *white symbols* negative BCC and *grey symbols* BCC with changing sign over time. N_{SIG} number of chronologies with significant trends; MV/SD: temporal changes of mean value and standard deviation, expressed in °C for temperature and mm for precipitation; *T* Temperature; *P* Precipitation; month is represented by a *number* (e.g. 1: January); *p* year before ring formation (year $n-1$). **b**, **c**, **d** Graphs detailing the temporal trends for three cases: temperature in April, temperature in July and precipitation in July, respectively. *Bold line* average trend amongst the 31 chronologies; *dashed lines* standard deviation (sd)

coefficient was significant at least one time per climatic regressor, with three of them presenting more than 50% of significant trends (T12p, T7 and P7). The overall proportion of significant temporal trends in BCC was slightly higher for temperature than for precipitation (28.2 and 24.7%, respectively).

For a given climatic regressor, the sign and the nature (either strengthening, or weakening, or changing in BCC sign over time) of the significant trends were similar amongst the chronologies (Fig. 6a).

The most frequent trends occurred during previous autumn (September to December), April and July (Fig. 6a). BCC with temperature in September and October changed from negative values at the beginning of the century to positive ones at the end. A similar pattern was also observed in April and July (Fig. 6b, c), whilst the opposite trend was evidenced in November and December, with BCC becoming negative over time. Considering precipitation, BCC changed from positive to negative values in November and July (Fig. 6d). The opposite tendency was highlighted in January and August when focussing on chronologies under oceanic conditions.

Discussion

Can a general pattern in climate-growth relationships be drawn?

As observed in previous studies (Lebourgeois et al. 2004, 2006; Friedrichs et al. 2009b; Dolezal et al. 2010), *Q. petraea* displayed a low climate sensitivity, with BCC being rarely significant and no single climatic regressor controlling radial growth. This could also explain the rather low percentage of inertia of the two first axes of PCA_{PY} and PCA_{BCC} (Figs. 3, 4). One hypothesis could be that environmental conditions of the forests under study were not too restrictive for tree growth. As a result of its high commercial value, *Q. petraea* was often favoured in contexts without strong ecological constraints to improve its growth and wood quality. Indeed, the sampled forests corresponded to low altitude and temperate climate associated with rather deep soils (at least on metre depth, except for the chronology *L* with 60 cm). Another explanation could be that the study area was located almost at the centre of the geographical distribution of the species (http://www.euforgen.org), so that the climate may be low limiting. Finally, the absence of a clear common pattern in sensitivity to climate might be related to the high genetic polymorphism amongst *Quercus* populations (Petit et al. 2002), which could induce inter-tree variability in response to climate, preventing us from drawing clear climate-growth relationships at the stand scale.

The most common response corresponded to negative correlation with temperature in March (Fig. 5a), whilst most of the previous investigations highlighted non-significant correlation throughout Europe (Lebourgeois et al. 2004; Cedro 2007; Friedrichs et al. 2009a, b; Dolezal et al. 2010). However, in the Swiss Alps, such a negative influence was found on the ring-porous species *Castanea sativa* (Fonti and Garcia-Gonzalez 2004; Fonti et al. 2007). In the latter study, the authors explained that a warm late winter could increase the cell sensitivity to auxin signal before bud burst, which resulted in smaller vessels later in the growth season as a consequence of an early and fast process of differentiation. A second hypothesis could be that an early bud burst due to warm late winter conditions led to higher risks of late frost damages (Ducousso et al. 1996).

Later in the season (May to July), radial growth was generally limited by water stress (Fig. 5). Even if weak, this relationship was nevertheless consistent with the pattern usually observed for this species (Lebourgeois et al. 2004; Friedrichs et al. 2009b; Dolezal et al. 2010). The analysis of the pointer years confirmed that summer drought was the main limiting factor of the radial growth (Fig. 3 and Online Resource 2). From the ecophysiological point of view, severe water stress significantly reduced cellular turgor (Thomas and Gausling 2000) and increased xylem embolism (Cochard et al. 1992), leading to a decrease in photosynthetic activity and growth.

The difficulty of drawing a general pattern (1) confirmed that this species displayed a general weak sensitivity to climate, and (2) proved that the climate-growth relationships highly varied along the longitudinal gradient, from oceanic to semi-continental conditions.

Spatial variation in sensitivity to climate

The sensitivity to water stress was higher under the driest and warmest conditions, i.e. under oceanic climate, with more negative BCC in July and August for temperature and more positive for precipitation. In the same way, the strength of positive correlations with precipitation from November to March decreased under fresh and wet conditions, highlighting that the role of previous year hydric conditions was more important under water limited environment (Lebourgeois et al. 2004; Zweifel et al. 2006; Cedro 2007) than under humid semi-continental climate (Friedrichs et al. 2009a).

Surprisingly, inverse relationships were pointed out in June, with a higher sensitivity to water stress under semi-continental climate (Fig. 5c). In the North-East of France, around 60–70% of the ring width of sessile oak is formed during June (Lebourgeois, personal communication), which could explain the high sensitivity to both temperature and precipitation. Under oceanic conditions, the rather low sensitivity in June compared to May has been previously observed by Lebourgeois et al. (2004), and could be linked to a more precocious radial growth. Indeed, sessile oak bud burst is delayed between 10 and 20 days from West to East (Lebourgeois et al. 2010a), which may progressively retard the maximum growth rate from May to June along the longitudinal gradient.

From previous October to February, the general trend consisted in an increasing positive correlation to temperature from West to East (Fig. 5a). Even if most of the BCC were non-significant (except in October), this pattern was consistent with the hypothesis of an increasing frost limitation under semi-continental conditions.

Temporal instability in sensitivity to climate

Spatial homogeneity in temporal trends

Moving correlations highlighted a general instability of climate-growth relationships over the 20th century. The signs and the natures of BCC trends were rather consistent amongst the chronologies (Fig. 6a), which contradicted the hypothesis of spatially dependent changes. In Germany, Friedrichs et al. (2009a) also pointed out synchronous instability between two oak species and various climatic contexts. In the present study, the homogeneity could be related to the similar climatic trends observed over the study area (Online Resource 3), tending to prove that the temporal variations under temperate conditions were a broad-scale phenomenon, with rather low modulations of climate-growth relationships instabilities by regional climatic differences.

Moderate consistency between sensitivity and climatic trends

The period 1914–1993 did not allow an analyse of the impact of the rising warming observed since the last three decades (Moisselin et al. 2002; Jones and Moberg 2003; Briffa et al. 2009). However, both MV and SD significantly changed over this period. Temperature became cooler and less variable during the growing season (except July) and September. At the same time, precipitation tended to increase with a greater inter-annual variability, except in July with a decrease of both MV and SD. Climatic trends were consistent with findings of Moisselin et al. (2002) for the entire France, who observed a downward trend of 0.7°C between 1940 and 1980, before a strong increase (+1.1°C between 1980 and 2000). The simultaneous variations of MV and SD prevented us from clearly separating the respective effects of both parameters on BCC instability.

The strongest independency between climatic and BCC trends was observed during the growing season, from May to July. The cooling and precipitation increase in May and June did not lead to a decrease in sensitivity to water stress. Similarly, BCC in July got closer to zero, with a sign inversion at the end of the period, although water stress tended to increase (Fig. 6). This independency seemed physiologically difficult to explain. It might be suggested that, under low-limiting temperate conditions the amelioration of the late spring water balance did not significantly modify the rather low sensitivity to climate in May and June. On the contrary, the decreasing drought-limitation in July could result from the increase of rainfall earlier in the growing season which offset the increasing evapo-transpiration demand linked to warming. Indeed, favourable hydric balance from March to June reduced soil water deficit in both intensity and duration (Lebourgeois et al. 2005), and may delay summer drought-induced cavitation (Tyree and Cochard 1996; Bréda et al. 2006), which was consistent with the increasing sensitivity to precipitation in August under the driest contexts (chronologies D to H). A second explanation of the decreasing correlation in July could be that sensitivity may depend on climatic variability: high inter-annual variability is expected to increase climatic anomalies and so the number of years during which climate limits or stimulates tree growth. Thus, it might be hypothesized that the decrease of the year-to-year variability of precipitation (significant reduction of SD) could result in a lower sensitivity.

Strong and common BCC trends were also observed in April in disagreement with previous findings in Europe which highlighted stability over the last century (Friedrichs et al. 2009a, b; Dolezal et al. 2010). The strong decrease of both MV and SD for temperature in April (−0.9 and −0.35°C respectively) was accompanied by a shift from negative to positive correlations for 18 chronologies amongst 31. As April conditions often determined phenological events (Nizinski and Saugier 1988; Lebourgeois et al. 2010a; Morin et al. 2010) and cambial reactivation (Rossi et al. 2007; Gruber et al. 2010), the chilling may have progressively delayed the beginning of the growing season, leading to positive correlation between temperature and ring width at the end of the study period.

Finally, significant BCC trends were pointed out during previous autumn, from September to December (Fig. 6a). Focusing on temperature, correlations changed from negative to positive values in September (and sometimes October), whilst the inverse trend was evidenced in November and December. Despite the difficulty to elucidate the ecophysiological mechanisms driving temporal instability during this season (D'Arrigo et al. 2008), such changes can highly modify ecosystem functioning and carbon sequestration (Piao et al. 2008). A cooler and more humid September followed by a warmer October might reduce both drought in late summer and frost in mid-autumn, leading to a longer growing season. Climate being less restrictive, trees began to respond positively to these new early autumn conditions. BCC trends also suggested that trees adjusted their response to warmer and more humid conditions during late autumn, mainly in November. The explanation of such instability appeared unclear, all the more since the climatic trends were non-significant. Previous studies showed that too warm winters can disrupt the physiological process linked to leaf phenology (Morin et al. 2010) and also modify the ratio between respiration and photosynthesis (Piao et al. 2008). Increasing respiration with increasing temperature during autumn and winter may partially consume carbohydrate reserves (Ogren 2000), which were initially stocked to support wood formation and leaves unfolding in spring (Barbaroux and Bréda 2002).

Conclusion

As expected, *Q. petraea* displayed a rather low sensitivity to climate. High temperature in March and water stress from May to July appeared to be the main growth limiting factors. The sensitivity to water stress generally decreased from oceanic to semi-continental conditions (except in June). Similarly, the positive correlations to precipitation from November to March generally decreased from West to East, whilst positive correlations to autumn and winter temperature tended to increase. These results confirmed that under fresh and humid conditions, the amount of water was a less important factor, whilst winter frost limitation slightly strengthened.

Most of the studies on the "divergence problem" pointed out instabilities which were related to global change (either increasing temperature at high elevations and latitudes or increasing aridity under Mediterranean context). Our analysis revealed instability in climate-growth relationships before the global warming observed since the middle of the 1980s. These great temporal variations in sensitivity under rather stable climatic conditions represented a deviation from the uniformitarian principle traditionally applied to dendroclimatology (Fritts 1976). Such multi-decadal instabilities in climate-growth relationships should be taken into account when using tree-ring as proxies for climate reconstructions.

Acknowledgments We gratefully thank the European Commission, the French Ministry for Agriculture and Fisheries (MAP), the National Institute for Agronomic Research (INRA) and the French Forest Service (ONF) for providing data and support to the present study. The first author was also funded by a PhD grant from the French Ministry of High Education and Scientific Research. We also wish to thank: M. Charru, R. Bertrand for their helpful discussions, and all people who took part to the field campaign. We acknowledge the editor's and reviewers' remarks which helped improving the article.

References

Andreu L, Gutiérrez E, Macias M, Ribas M, Bosch O, Camarero JJ (2007) Climate increases regional tree-growth variability in Iberian pine forests. Glob Change Biol 13(4):804–815. doi:10.1111/j.1365-2486.2007.01322.x

Barbaroux C, Bréda N (2002) Contrasting distribution and seasonal dynamics of carbohydrate reserves in stem wood of adult ring-porous sessile oak and diffuse-porous beech trees. Tree Physiol 22(17):1201–1210. doi:10.1093/treephys/22.17.1201

Becker M (1989) The role of climate on present and past vitality of silver fir forests in the Vosges Mountains of northeastern France. Can J For Res 19(9):1110–1117. doi:10.1139/x89-168

Becker M, Nieminen TM, Gérémia F (1994) Short-term variations and long-term changes in oak productivity in northeastern France—the role of climate and atmospheric CO2. Ann Sci For 51(5):477–492. doi:10.1051/forest:19940504

Benichou P, Le Breton O (1987) Prise en compte de la topographie pour la cartographie des champs pluviométriques statistiques. La Météorol 7(19):23–34

Bergès L, Dupouey JL, Franc A (2000) Long-term changes in wood density and radial growth of *Quercus petraea* Liebl in northern France since the middle of the nineteenth century. Trees Struct Funct 14(7):398–408. doi:10.1007/s004680000055

Biondi F (1997) Evolutionary and moving response functions in dendroclimatology. Dendrochronologia 15:139–150

Bréda N, Huc R, Granier A, Dreyer E (2006) Temperate forest trees and stands under severe drought: a review of ecophysiological responses, adaptation processes and long-term consequences. Ann Sci For 63(6):625–644. doi:10.1051/forest:2006042

Briffa KR, van der Schrier G, Jones PD (2009) Wet and dry summers in Europe since 1750: evidence of increasing drought. Int J Climatol 29(13):1894–1905. doi:10.1002/joc.1836

Bunn AG (2008) A dendrochronology program library in R (dplR). Dendrochronologia 26(2):115–124. doi:10.1016/j.dendro.2008.01.002

Cedro A (2007) Tree-ring chronologies of downy oak (*Quercus pubescens*), pedunculate oak (*Q-robur*) and sessile oak (*Q-petraea*) in the Bielinek Nature Reserve: comparison of the climatic determinants of tree-ring width. Geochronometria 26:39–45. doi:10.2478/v10003-007-0005-2

Cochard H, Bréda N, Granier A, Aussenac G (1992) Vulnerability to air embolism of three European oak species (*Quercus petraea* (Matt) Liebl, *Q. pubescens* Willd, *Q. robur* L). Ann Sci For 49(3):225–233. doi:10.1051/forest:19920302

Cook ER, Kairiukstis LAE (1990) Methods of dendrochronology: applications in the environmental sciences. Kluwer Academic Publishers, Dordrecht, Boston, London

Cook ER, Peters K (1981) The smoothing spline: a new approach to standardizing forest interior tree-ring width series for dendroclimatic studies. Tree-Ring Res 41:45–53

D'Arrigo R, Wilson R, Liepert B, Cherubini P (2008) On the 'Divergence Problem' in northern forests: a review of the tree-ring evidence and possible causes. Glob Planet Change 60(3–4):289–305. doi:10.1016/j.gloplacha.2007.03.004

Davi H, Dufrêne E, François C, Le Maire G, Loustau D, Bosc A, Rambal S, Granier A, Moors E (2006) Sensitivity of water and carbon fluxes to climate changes from 1960 to 2100 in European forest ecosystems. Agric For Meteorol 141(1):35–56. doi:10.1016/j.agrformet.2006.09.003

Di Filippo A, Biondi F, Cufar K, de Luis M, Grabner M, Maugeri M, Saba EP, Schirone B, Piovesan G (2007) Bioclimatology of beech (*Fagus sylvatica* L.) in the Eastern Alps: spatial and altitudinal climatic signals identified through a tree-ring network. J Biogeogr 34(11):1873–1892. doi:10.1111/j.1365-2699.2007.01747.x

Dittmar C, Zech W, Elling W (2003) Growth variations of Common beech (*Fagus sylvatica* L.) under different climatic and environmental conditions in Europe—a dendroecological study. For Ecol Manag 173(1–3):63–78. doi:10.1016/S0378-1127(01)00816-7

Dolezal J, Mazurek P, Klimesova J (2010) Oak decline in southern Moravia: the association between climate change and early and late wood formation in oaks. Preslia 82(3):289–306

Ducousso A, Guyon JP, Kremer A (1996) Latitudinal and altitudinal variation of bud burst in western populations of sessile oak (*Quercus petraea* (Matt) Liebl). Ann Sci For 53(2–3):775–782. doi:10.1051/forest:19960253

Duplat P, Tran-Ha M (1997) Modelling the dominant height growth of sessile oak (*Quercus petraea* Liebl) in France. Inter-regional variability and effect of the recent period (1959–1993). Ann Sci For 54(7):611–634. doi:10.1051/forest:19970703

Fonti P, Garcia-Gonzalez I (2004) Suitability of chestnut earlywood vessel chronologies for ecological studies. New Phytol 163(1):77–86. doi:10.1111/j.1469-8137.2004.01089.x

Fonti P, Solomonoff N, Garcia-Gonzalez I (2007) Earlywood vessels of *Castanea sativa* record temperature before their formation. New Phytol 173(3):562–570. doi:10.1111/j.1469-8137.2006.01945.x

Friedrichs DA, Büntgen U, Frank DC, Esper J, Neuwirth B, Loffler J (2009a) Complex climate controls on 20th century oak growth in Central-West Germany. Tree Physiol 29(1):39–51. doi:10.1093/treephys/tpn003

Friedrichs DA, Trouet V, Büntgen U, Frank DC, Esper J, Neuwirth B, Loffler J (2009b) Species-specific climate sensitivity of tree growth in Central-West Germany. Trees Struct Funct 23(4):729–739. doi:10.1007/s00468-009-0315-2

Fritts HC (1976) Tree rings and climate. Academic Press, London, New York, San Francisco

Gaussen H, Bagnouls F (1952) L'indice xérothermique. Bull de l'Assoc des Géogr Fr 222–223(jan-fév):10–16

Gruber A, Strobl S, Veit B, Oberhuber W (2010) Impact of drought on the temporal dynamics of wood formation in *Pinus sylvestris*. Tree Physiol 30(4):490–501. doi:10.1093/treephys/tpq003

Guiot J (1991) The bootstrapped response function. Tree-Ring Bull 51:39–41

Hughes MK (2002) Dendrochronology in climatology—the state of the art. Dendrochronologia 20:95–116. doi:10.1078/1125-7865-00011

Jones PD, Moberg A (2003) Hemispheric and large-scale surface air temperature variations: an extensive revision and an update to 2001. J Clim 16(2):206–223. doi:10.1175/1520-0442(2003)016<0206:HALSSA>2.0.CO;2

Kelly PM, Leuschner HH, Briffa KR, Harris IC (2002) The climatic interpretation of pan-European signature years in oak ring-width series. Holocene 12(6):689–694. doi:10.1191/0959683602hl582rp

Lebourgeois F (1997) RENECOFOR—Etude dendrochronologique des 102 peuplements du réseau

Lebourgeois F (2006) Sensibilité au climat des Chênes sessile et pédonculé dans le réseau RENECOFOR. Comparaison avec les hêtraies. Rev For Fr 53(1):29–44

Lebourgeois F, Cousseau G, Ducos Y (2004) Climate-tree-growth relationships of *Quercus petraea* Mill. stand in the Forest of Berce ("Futaie des Clos", Sarthe, France). Ann Sci For 61(4):361–372. doi:10.1051/forest:2004029

Lebourgeois F, Bréda N, Ulrich E, Granier A (2005) Climate-tree-growth relationships of European beech (*Fagus sylvatica* L.) in the French Permanent Plot Network (RENECOFOR). Trees Struct Funct 19(4):385–401. doi:10.1007/s00468-004-0397-9

Lebourgeois F, Pierrat JC, Perez V, Piedallu C, Cecchini S, Ulrich E (2010a) Simulating phenological shifts in French temperate forests under two climatic change scenarios and four driving global circulation models. Int J Biometeorol 54(5):563–581. doi:10.1007/s00484-010-0305-5

Lebourgeois F, Rathgeber CKB, Mérian P, Ulrich E (2010b) Sensitivity of French temperate forests to climate variability and extreme events: example of the French Network RENECOFOR. In: Edytem (ed) Panorama de la dendrochronologie en France, Dignes-les-Bains, 17 October 2009, pp 19–26

Legendre P, Legendre L (1998) Numerical ecology. Elsevier, New York

Lindner M, Maroschek M, Netherer S, Kremer A, Barbati A, Garcia-Gonzalo J, Seidl R, Delzon S, Corona P, Kolstrom M, Lexer MJ, Marchetti M (2010) Climate change impacts, adaptive capacity, and vulnerability of European forest ecosystems. For Ecol Manag 259(4):698–709. doi:10.1016/j.foreco.2009.09.023

Macias M, Andreu L, Bosch O, Camarero JJ, Gutiérrez E (2006) Increasing aridity is enhancing silver fir (*Abies alba* mill.) water stress in its south-western distribution limit. Clim Change 79(3–4):289–313. doi:10.1007/s10584-006-9071-0

Mérian P, Lebourgeois F (2011) Size-mediated climate-growth relationships in temperate forests: a multi-species analysis. For Ecol Manag 261(8):1382–1391. doi:10.1016/j.foreco.2011.01.019

Misson L, Rathgeber C, Guiot J (2004) Dendroecological analysis of climatic effects on *Quercus petraea* and *Pinus halepensis* radial growth using the process-based MAIDEN model. Can J For Res 34(4):888–898. doi:10.1139/X03-253

Moberg A, Jones PD (2005) Trends in indices for extremes in daily temperature and precipitation in central and western Europe, 1901–99. Int J Climatol 25(9):1149–1171. doi:10.1002/joc.1163

Moisselin JM, Schneider M, Canellas C, Mestre O (2002) Les changements climatiques en France au XXème siècle. Etude des longues séries homogénéisées de données de température et de précipitations. La Météorol 38:45–56

Morin X, Roy J, Sonie L, Chuine I (2010) Changes in leaf phenology of three European oak species in response to experimental climate change. New Phytol 186(4):900–910. doi:10.1111/j.1469-8137.2010.03252.x

Myers JL, Well AD (2003) Research design and statistical analysis, 2nd edn. Routledge Academic, New York

Nizinski JJ, Saugier B (1988) A model of leaf budding and development for a mature *Quercus* forest. J Appl Ecol 25(2):643–652

Ogren E (2000) Maintenance respiration correlates with sugar but not nitrogen concentration in dormant plants. Physiol Plant 108(3):295–299. doi:10.1034/j.1399-3054.2000.108003295.x

Petit RJ, Csaikl UM, Bordacs S, Burg K, Coart E, Cottrell J, van Dam B, Deans JD, Dumolin-Lapegue S, Fineschi S, Finkeldey R, Gillies A, Glaz I, Goicoechea PG, Jensen JS, Konig AO, Lowe AJ, Madsen SF, Matyas G, Munro RC, Olalde M, Pemonge MH, Popescu F, Slade D, Tabbener H, Taurchini D, de Vries SGM, Ziegenhagen B, Kremer A (2002) Chloroplast DNA variation in European white oaks—phylogeography and patterns of diversity based on data from over 2600 populations. For Ecol Manag 156(1–3):5–26. doi:10.1016/S0378-1127(01)00645-4

Piao SL, Ciais P, Friedlingstein P, Peylin P, Reichstein M, Luyssaert S, Margolis H, Fang JY, Barr A, Chen AP, Grelle A, Hollinger DY, Laurila T, Lindroth A, Richardson AD, Vesala T (2008) Net carbon dioxide losses of northern ecosystems in response to autumn warming. Nature 451(7174):49–52. doi:10.1038/nature06444

Piovesan G, Biondi F, Bernabei M, Di Filippo A, Schirone B (2005) Spatial and altitudinal bioclimatic zones of the Italian peninsula identified from a beech (*Fagus sylvatica* L.) tree-ring network. Int J Ecol 27(3):197–210. doi:10.1016/j.actao.2005.01.001

R Development Core Team (2010) R: a language and environment for statistical computing. R Foundation for Statistical Computing, Vienna, Austria. ISBN: 3-900051-07-0, URL http://www.R-project.org

Rossi S, Deslauriers A, Anfodillo T, Carraro V (2007) Evidence of threshold temperatures for xylogenesis in conifers at high altitudes. Oecologia 152(1):1–12. doi:10.1007/s00442-006-0625-7

Rotzer T, Grote R, Pretzsch H (2005) Effects of environmental changes on the vitality of forest stands. Eur J For Res 124(4):349–362. doi:10.1007/s10342-005-0086-2

Rozas V (2005) Dendrochronology of pedunculate oak (*Quercus robur* L.) in an old-growth pollarded woodland in northern Spain: tree-ring growth responses to climate. Ann Sci For 62(3):209–218

Schweingruber FH (1996) Tree rings and environment: Dendroecology. Swiss Federal Institute for Forest, Snow and Landscape Research, and Paul Haupt Verlag, Bern

Tardif J, Camarero JJ, Ribas M, Gutierrez E (2003) Spatiotemporal variability in tree growth in the Central Pyrenees: climatic and site influences. Ecol Monogr 73(2):241–257. doi:10.1890/0012-9615(2003)073[0241:SVITGI]2.0.CO;2

Tessier L, Nola P, Serre-Bachet F (1994) Deciduous *Quercus* in the Mediterranean region: tree-ring/climate relationships. New Phytol 126(2):355–367. doi:10.1111/j.1469-8137.1994.tb03955.x

Thomas FM, Gausling T (2000) Morphological and physiological responses of oak seedlings (*Quercus petraea* and *Q. robur*) to moderate drought. Ann Sci For 57(4):325–333

Tyree MT, Cochard H (1996) Summer and winter embolism in oak: impact on water relations. Ann Sci For 53(2–3):173–180. doi:10.1051/forest:19960201

Weber P, Bugmann H, Rigling A (2007) Radial growth responses to drought of *Pinus sylvestris* and *Quercus pubescens* in an inner-Alpine dry valley. J Veg Sci 18(6):777–792. doi:10.1111/j.1654-1103.2007.tb02594.x

Wigley TM, Briffa KR, Jones PD (1984) On the average value of correlated time series, with applications in dendroclimatology and hydrometeorology. J Clim Appl Meteorol 23:201–213. doi:10.1175/1520-0450(1984)023<0201:OTAVOC>2.0.CO;2

Zang C (2009) bootRes: bootstrapped response and correlation functions. R package version 02. http://CRANR-projectorg/package=bootRes

Zweifel R, Zimmermann L, Zeugin F, Newbery DM (2006) Intra-annual radial growth and water relations of trees: implications towards a growth mechanism. J Exp Bot 57(6): 1445–1459. doi:10.1093/jxb/erj125